Chapter 7

Calcium Signaling Initiated by Agonists in Mesenchymal Stromal Cells from the Human Adipose Tissue

Polina D. Kotova, Olga A. Rogachevskaja, Marina F. Bystrova, Ekaterina N. Kochkina, Denis S. Ivashin and Stanislav S. Kolesnikov

Additional information is available at the end of the chapter

http://dx.doi.org/10.5772/intechopen.79097

Abstract

Mesenchymal stromal cells (MSCs) from different sources represent a heterogeneous population of proliferating non-differentiated cells that contain multipotent stem cells capable of originating a variety of mesenchymal cell lineages. By using Ca^{2+} imaging and the Ca^{2+} dye $Fluo^{-4}$, we studied MSCs from the human adipose tissue and examined Ca^{2+} signaling initiated by a variety of GPCR ligands, focusing primarily on adrenergic and purinergic agonists. Being characterized by a relative change of $Fluo^{-4}$ fluorescence, agonist-induced Ca^{2+} responses were generated in an "all-or-nothing" fashion. Specifically, at relatively low doses, agonists elicited undetectable responses but initiated quite similar Ca^{2+} transients at all concentrations above the threshold. The inhibitory analysis and Ca^{2+}/IP^3 uncaging pointed at the phosphoinositide cascade as a pivotal pathway responsible for agonist transduction and implicated Ca^{2+}-induced Ca^{2+} release (CICR) in shaping agonists-dependent Ca^{2+} signals. Altogether, our data suggest that agonist transduction in MSCs includes two fundamentally different stages: an agonist initially triggers a local, gradual, and relatively small Ca^{2+} signal, which next stimulates CICR to accomplish transduction with a large and global Ca^{2+} transient. By involving the trigger-like mechanism CICR, a cell is capable of generating Ca^{2+} responses of virtually universal shape and magnitude at different agonist concentrations above the threshold.

Keywords: Ca^{2+} signaling, G-protein coupled receptors, calcium-induced calcium release, IP_3 receptors, mesenchymal stromal cells, adipose tissue

1. Introduction

Mesenchymal stromal cells (MSCs) are described as a heterogeneous cellular pool that includes immature cells responsible for the replenishment of supportive and connective tissues due to their capability of maintaining self-renewal and multipotent differentiation [1–3]. By unique biologic properties, cultured MSCs from different sources attract sufficient interest in the fields of regenerative medicine and immunotherapy [4–6]. Despite evident progress in MSC biology spurred by the therapeutic potential of these cells, current knowledge on their receptor and signaling systems remains scarce. Evidence exists that MSCs are capable of sensing complex extracellular cues, including hormones, cytokines, and nucleotides [7, 8]. This implies that MSCs employ multiple surface receptors and signaling pathways to adjust their physiological functions to specific tissue microenvironment.

Here, we studied MSCs derived from the human adipose tissue and examined Ca^{2+} signaling initiated by a variety of agonists of G-protein coupled receptors (GPCRs). We specifically focused on adrenergic and purinergic signaling systems that attracted us for the following reasons. It has been known for a long time that noradrenaline released by sympathetic nerves regulates distinct physiological processes in the adipose tissue such as lipid and glucose metabolism and secretion of distinct signaling molecules, including adipocytokines and cytokines [9]. Hence, MSCs that reside in the adipose tissue can be subjected to the action of noradrenaline and factors released by adipocytes on adrenergic stimulation. Purinergic agonists have been documented as an important factor determining MSC fate [7, 8, 10–12]. Reportedly, ATP serves both as an adipogenic regulator and an osteogenic factor, while its downstream product adenosine switches off adipogenic differentiation and promotes osteogenesis [13, 14]. Damaged tissues are an abundant source of extracellular ATP that may be converted by extracellular nucleotidases to ADP and eventually to adenosine [15]. It therefore might be expected that MSCs are exposed to and regulated by nucleotides and adenosine when these cells migrate *in vivo* or are transplanted *ex vivo* into an injured tissue.

The responsiveness to purines and pyrimidines is widespread among eukaryotic cells, which express numerous purinoreceptors from the P1 and P2 families. The P1 subgroup includes four G-protein-coupled receptors (A_1, A_{2A}, A_{2B}, A_3) recognizing adenosine as an endogenous agonist [16]. The more diverse P2 family is composed of ionotropic P2X and metabotropic P2Y receptors. P2X receptors are cationic channels specifically gated by ATP, while P2Y receptors are activated by multiple purine and pyrimidine nucleotides or by sugar nucleotides and couple to intracellular second messenger pathways by heteromeric G proteins [17, 18]. In mammals, seven genes encode P2X subunits ($P2X_{1–7}$) that can form homo- and heterotrimeric cation channels with noticeable Ca^{2+} permeability [19, 20]. The P2Y subfamily includes eight members ($P2Y_{1,2,4,6,11,12,13,14}$), which are distinct by ligand specificity and coupling to downstream signaling pathways, including the ubiquitous phosphoinositide cascade [17, 18].

Nine genes encode human adrenoreceptors, which all belong to the GPCR superfamily and compose three distinctive subgroups, including three α_1 (α_{1A}, α_{1B}, α_{1D}), three α_2 (α_{2A}, α_{2B}, α_{2C}), and three β (β_1, β_2, β_3) receptor subtypes. Canonically, α_1-adrenoreceptors couple to G_q and

are ubiquitously involved in Ca^{2+} signaling [21]. Although α_2 isoforms widely regulate adenylyl cyclase via G_i, their coupling to phospholipase C (PLC) and Ca^{2+} mobilization has also been documented [22]. All three β-subtypes are linked to adenylyl cyclase by G_s, although β_2 and β_3 also couple to G_i, and directly do not control intracellular Ca^{2+} [23]. Given that certain isoforms of adrenergic and purinergic receptors are coupled to Ca^{2+} mobilization in diverse cell types, we considered Ca^{2+} imaging as an adequate approach to detail purinergic and adrenergic transduction in MSCs.

2. Materials and methods

2.1. Cell isolation and culturing

MSCs of the first passage were obtained from the Faculty of Basic Medicine at Lomonosov Moscow State University. All procedures that involved human participants were performed in accordance with the ethical standards approved by the Bioethical Committee of the Faculty based on the 1964 Helsinki declaration and its later amendments. The study involved 21 healthy (not suffered from infectious or systemic diseases and malignancies) individuals from 21 to 55 years old, and informed consent was obtained from each participant.

Cells were isolated from subcutaneous fat tissue of healthy donors using enzymatic digestion as previously described [24]. Briefly, the adipose tissue was extensively washed with two volumes of Hank's Balanced Salt Solution (HBSS) containing 5% antibiotic/antimycotic solution (10,000 units of penicillin, 10,000 μg of streptomycin, and 25 μg of Amphotericin B per mL; HyClone), fragmented, and then digested at 37°C for 1 h in the presence of collagenase (200 U/ml, Sigma-Aldrich) and dispase (10 U/ml, BD Biosciences). Enzymatic activity was neutralized by adding an equal volume of culture medium (HyClone™ AdvanceSTEM™ Mesenchymal Stem Cell Basal Medium for human undifferentiated mesenchymal stem cells containing 10% of HyClone™ AdvanceSTEM™ Mesenchymal Stem Cell Growth Supplement (CGS), 1% antibiotic/antimycotic solution (HyClone) and centrifuged at 200 g for 10 min. This led to the sedimentation of diverse cells, including MSCs, macrophages, lymphocytes, and erythrocytes, unlike adipocytes that remained floating. After removal of supernatant, a lysis solution (154 mM NH_4Cl, 10 mM $KHCO_3$, and 0.1 mM EDTA) was added to a cell pellet to lyse erythrocytes, and cell suspension was centrifuged at 200 g for 10 min. Sedimented cells were resuspended in the MSC culture medium and filtered through a 100-μm nylon cell strainer (BD Biosciences). As indicated by flow [24], after isolation and overnight preplating, the obtained cell population contained not only MSC cells that basically represented the most abundant subgroup but also admixed macrophages and lymphocytes. The two last cell subgroups were dramatically depleted by culturing for a week in the MSC culture medium and humidified atmosphere (5% CO_2) at 37°C. The obtained MSC population was maintained at a subconfluent level (~80% confluency) and passaged using HyQTase (HyClone). By using the methodology described previously [25], cultured cells were demonstrated to differentiate into the osteogenic, chondrogenic, and adipogenic directions, the finding confirming their multipotency. In experiments, MSCs of the second to fourth passages were usually used.

2.2. Preparation of cells for Ca^{2+} imaging

Before assaying with Ca^{2+} imaging, cells were maintained in a 12-socket plate for 12 h in the medium described above but without antibiotics. For isolation, cells cultured in a 1-ml socket were rinsed twice with the Versene solution (Sigma-Aldrich) that was then substituted for 200 μl HyQTase solution (HyClone) for 3–5 min. The enzymatic treatment was terminated by the addition of a 0.8 ml culture medium to a socket. Next, cells were resuspended, put into a tube, and centrifuged at 50 g for 45 s for moderate sedimentation. Isolated cells were collected by a plastic pipette and plated onto a photometric chamber of nearly 150 μl volume. The last was a disposable coverslip (Menzel-Glaser) with attached ellipsoidal resin wall. The chamber bottom was coated with Cell-Tak (BD Biosciences), enabling strong cell adhesion. Attached cells were then loaded with dyes for 20 min at room temperature (23–25°C) by adding Fluo-4 AM (4 μM) and Pluronic (0.02%; all from Molecular Probes) to a bath solution. Loaded cells were rinsed with the bath solution for several times and kept at 4°C for 1 h prior to recordings. Generally, incubation of MSCs at low temperature stabilized intracellular Ca^{2+} and decreased a fraction of spontaneously oscillating cells.

2.3. Ca^{2+} imaging and uncaging

Experiments were carried out using an inverted fluorescent microscope Axiovert 135 equipped with an objective Plan NeoFluar 20x/0.75 (Zeiss) and a digital EMCCD camera LucaR (Andor Technology). Apart from a transparent light illuminator, the microscope was equipped with a handmade system for epi-illumination via an objective. The epi-illumination was performed using a bifurcational glass fiber. One channel was used for Fluo-4 excitation and transmitted irradiation of a computer-controllable light-emitting diode (LED) LZ1-00B700H (LED Engin). LED emission was filtered with an optical filter ET480/20x (Chroma Technology). Fluo-4 emission was collected at 535 ± 25 nm by using an emission filter ET535/50 m (Chroma Technology). Serial fluorescent images were usually captured every second and analyzed using Imaging Workbench 6 software (INDEC). Within the 1-s acquisition period, the 480 nm LED was switched on for only 200 ms, during which cell fluorescence was collected. This protocol allowed for minimizing photobleaching of Fluo-4 at a sufficiently high signal-to-noise ratio achievable by adjusting LED emission. This enabled us to reliably assay cell responsiveness to different compounds applied serially for up to 60 min. Deviations of cytosolic Ca^{2+} from the resting level were quantified by a relative change in the intensity of Fluo-4 fluorescence ($\Delta F/F_0$) recorded from an individual cell.

Another channel was connected to a pulsed solid laser TECH-351 Advanced (680 mW) (Laser-Export, Moscow). This unit operated in a two harmonic mode and generated not only 351 nM UV light used for Ca^{2+} uncaging but also visible light at 527 nm. The last could penetrate into an emission channel through nonideal optical filters and elicit optical artifacts during uncaging. For Ca^{2+} or IP_3 uncaging, cells were loaded with 4 μM Fluo-4-AM (Invitrogen) and 4 μM NP-EGTA-AM (Invitrogen) or 4 μM caged-Ins(145)P3/PM (SiChem) + 0.02% Pluronic (Invitrogen) for 30 min at 23°C. The basic bath solution contained (mM): 110 NaCl, 5.5 KCl, 2 $CaCl_2$, 0.8 $MgSO_4$, 10 glucose, 10 HEPES-NaOH, and pH 7.4 (≈270 Osm). When necessary, 2 mM $CaCl_2$ in the bath was replaced with 0.5 mM EGTA + 0.4 mM $CaCl_2$, thus reducing free Ca^{2+} to nearly 260 nM at 23°C as calculated with the Maxchelator program (http://maxchelator.

stanford.edu). In this low Ca^{2+} bath solution, the glucose concentration was increased to 13 mM to keep osmolarity. All chemicals used in experiments described below were applied by the complete replacement of the bath solution in a 150-μl photometric chamber for nearly 2 s using a perfusion system driven by gravity. The used salts and buffers were from Sigma-Aldrich, and agonists and inhibitors were from Tocris.

3. Results

In a typical experiment, nearly a hundred of MSCs loaded with Fluo-4 resided in a photometric camera, and their responsiveness to different ligands was assayed with Ca^{2+} imaging. Consistently with observations of others [3], functional heterogeneity was characteristic of a MSC population derived from each particular donor. Although a variety of GPCR agonists were found to stimulate Ca^{2+} signaling in MSCs, including ATP, ADP, noradrenaline or adrenaline, acetylcholine or its analog carbachol, GABA, glutamate, serotonin, and UTP, only a relatively small group of cells in a given MSC population was specifically responsive to a particular agonist (**Figure 1**). Overall, nearly 10^3 MSCs were sequentially stimulated by multiple agonists applied at different combinations, and a particular cell was either irresponsive to all stimuli or responded to one, rarely two, particular compound (**Figure 1A–C**). ATP-sensitive cells composed the most abundant subgroup of 9–15% (12% on average), depending on MSC preparation (**Figure 1B**). The percentage of cells responsive to other agonists was on average: ADP—7.1, adenosine—8.7, carbachol—3.4, GABA—5, glutamate—1.2, noradrenaline—6.7, serotonin—6.6, and UTP—6 (**Figure 1B**). The more or less accurate analysis of distribution of MSC responsivity was performed for nucleotides. In designated experiments, wherein cells were sequentially stimulated by ATP, ADP, and UTP, 125 purinergic MSCs were assayed overall, and only 13 cells (10%) were found to respond to all three agonists at the indicated concentrations (**Figure 1C**). Both ATP and ADP stimulated Ca^{2+} signaling in 40 cells (32%) that did not respond to UTP; 33 cells (26%) preferred the ATP-UTP pair. In addition, 20, 9, and 7 cells (16, 7, and 6%) responded exclusively to ATP, ADP, or UTP, respectively (**Figure 1C**).

Thus, the results presented above (**Figure 1**) clearly demonstrated that responsiveness to a given agonist varied from cell to cell. Note that GPCRs from most subfamilies, e.g. P2Y receptors, can couple to several signaling pathways, depending on cellular context [26–29]. Hence, in cells nonresponsive in terms of Ca^{2+} signaling to a particular agonist, appropriate GPCRs might be either not expressed or not coupled to Ca^{2+} mobilization.

3.1. Dose dependence of MSC responses to adrenergic and purinergic agonists

In the present study, we focused on transduction of adrenergic and purinergic agonists capable of stimulating Ca^{2+} signaling in the MSC cytoplasm. We first aimed at evaluating dose dependencies of cellular responses to tested agonists. The analysis, which initially involved adrenergic transduction, revealed that Ca^{2+} responses varied with noradrenaline concentration in an "all-or-nothing" fashion. In other words, noradrenaline never caused detectable effects, when applied below 100 nM, but above the threshold of 100–200 nM, it elicited marked Ca^{2+} transients that were similarly shaped irrespective of agonist concentration (**Figure 2A**).

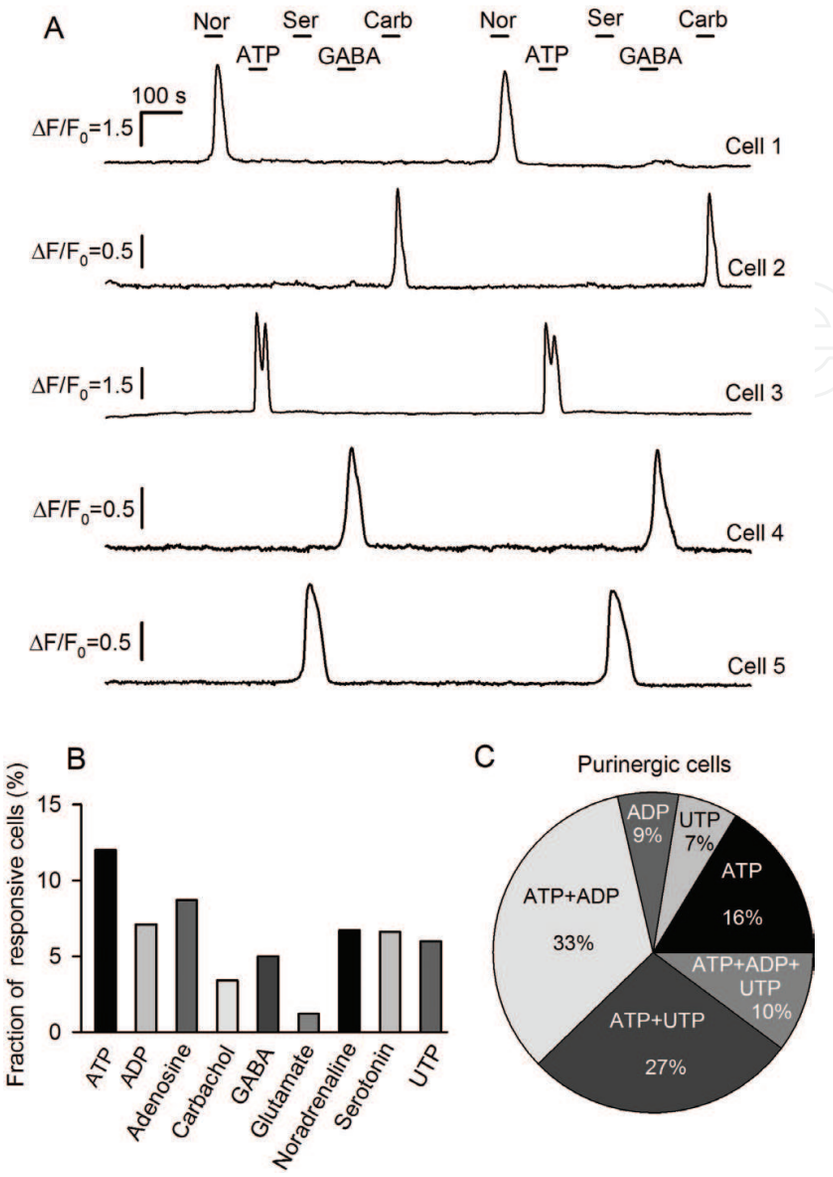

Figure 1. Functional heterogeneity of MSCs from the human adipose tissue. (A) Concurrent monitoring of intracellular Ca^{2+} in five different cells loaded with Fluo-4. The selected agonists were applied as indicated by the horizontal lines above the upper trace. (B) Fractional distribution of 426 MSCs that responded to at least one from the following serially applied agonists, including 10 μM ATP (adenosine triphosphate), 3 μM ADP (adenosine diphosphate), 10 μM adenosine (Adeno), 20 μM carbachol (carb), 20 μM GABA (gamma-aminobutyric acid), 10 μM glutamic acid (Glut), 0.5 μM noradrenaline (Nor), 10 μM serotonin (Ser), and 10 μM UTP (uridine triphosphate). (C) Distribution of MSC responsiveness to sequentially applied ATP (3 μM), ADP (3 μM), and UTP (10 μM) among a population of 125 cells, each being sensitive to at least one nucleotide.

Since we expected to obtain a somewhat gradual dose dependence, we considered the possibility that at concentrations used, noradrenaline might elicit too high Ca^{2+} transients, which all saturated Fluo-4 fluorescence, thus appearing alike. However, the permeabilizing agent saponin (0.1 mg/mL) evoked marked Ca^{2+} signals that exceeded noradrenaline responses by the factor of 1.5–2 (17 cells; **Figure 2A**). These observations indicated conclusively that MSC responses to varied noradrenaline could not be equalized due to saturation of the Ca^{2+} dye. The further analysis of MSC responsivity pointed out that the "all-or-nothing" phenomenon

http://dx.doi.org/10.5772/intechopen.79097

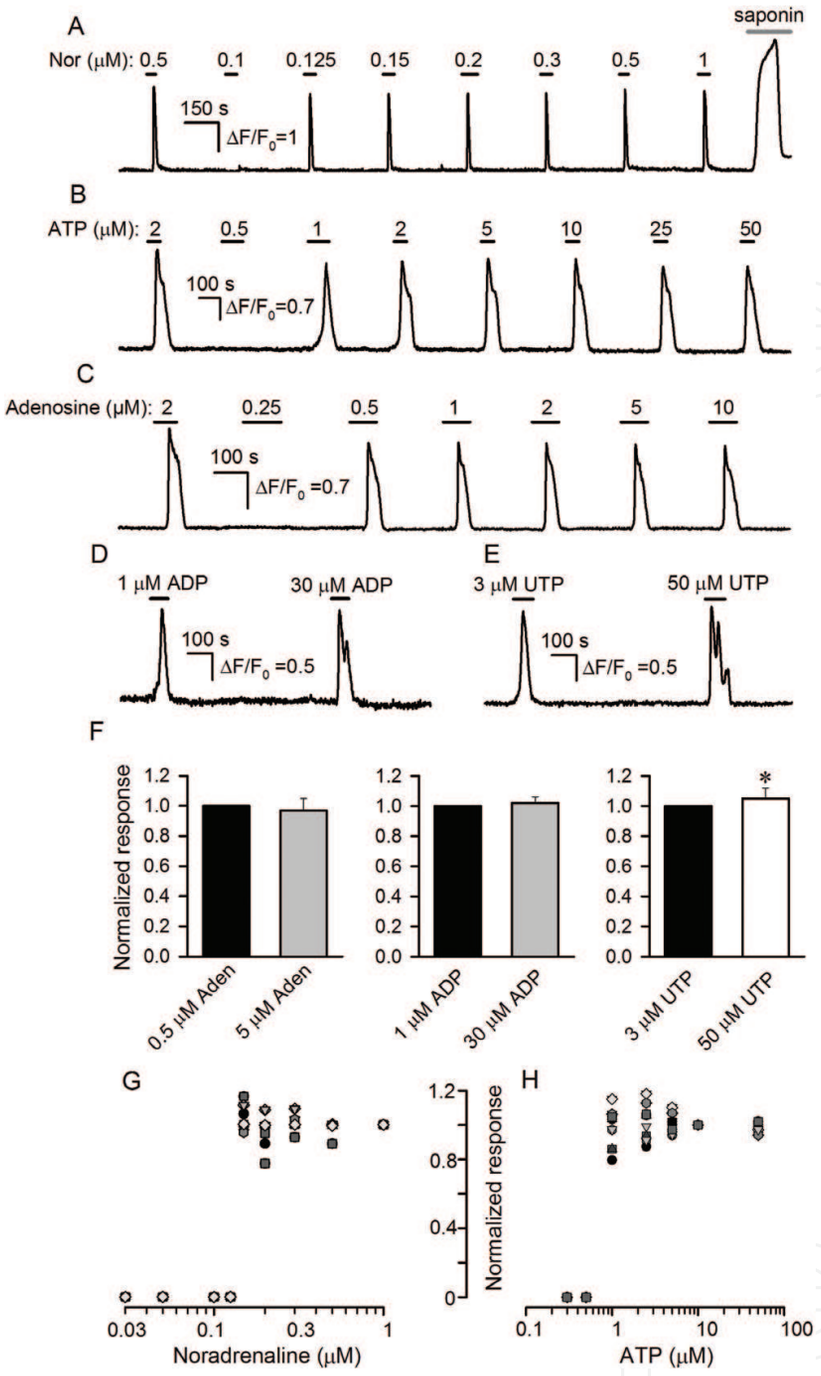

Figure 2. Agonists evoke Ca^{2+} responses in an "all-or-nothing" manner. (A–E) Monitoring of intracellular Ca^{2+} in five different MSCs serially stimulated by noradrenaline (A), ATP (B), ADP (C), UTP (D), and adenosine (E) at varied concentrations as indicated. In A, 0.1 mg/ml saponin was applied (arrow) in the end of the recording to demonstrate that Fluo-4 fluorescence was not saturated by Ca^{2+} bursts elicited by noradrenaline. (F) Summary of MSC responses to adenosine (n = 21; left panel), ADP (n = 16; middle panel) cells, and UTP (n = 11; right panel). For each assayed cell, a response to a particular agonist at low concentration was taken equal 1. The data are presented as mean ± S.D. The difference between responses to adenosine at 0.5 and 5 μM and to ADP at 1 and 30 μM ADP is statistically insignificant (student t-test, $p < 0.05$). The asterisk indicates significant difference ($p < 0.05$) of UTP responses at 3 and 50 μM. (G) Superimposed dose dependences of noradrenaline responses recorded from 10 cells that exhibited the threshold of 150 nM. For each cell, serial noradrenaline responses were normalized to a response to 1 μM noradrenaline. (H) Superimposed dose dependences of ATP responses recorded from eight cells that exhibited the threshold of 1 μM. In each case, ATP responses were normalized to a response to 10 μM ATP. In (G) and (H), each particular symbol corresponds to an individual cell.

was intrinsic for the agonist-dependent Ca^{2+} signaling in general, including purinergic transduction. In particular, submicromolar ATP was ineffective, while the nucleotide elicited Ca^{2+} transients in the MSC cytoplasm at 1–2 μM and higher (**Figure 2B**). The adenosine responses were characterized by the threshold of 0.2–0.3 μM and were similarly shaped at higher concentrations (9 cells; **Figure 2C**). For ADP- and UTP-responses, the threshold concentrations ranged within 0.5–2 and 3–6 μM, respectively. Although we did not carefully characterize MSC responses to adenosine, ADP, and UTP at widely and gradually varied concentrations, it appeared that dose-response curves for these agonists were also step-like. For example, Ca^{2+} transients of close magnitudes were usually elicited by adenosine at 0.5 and 5 μM (21 cells), ADP at 1 and 30 μM (16 cells), and UTP at 3 and 50 μM (11 cells) (**Figure 2C–F**).

In the case of noradrenaline and ATP, the dose dependence of MSC responses was carefully evaluated in designated experiments, wherein an agonist dose was gradually varied in a wide range of concentrations (**Figure 2A**, **B**). During this prolonged assay, responsiveness of many cells was liable to rundown, thus impeding the quantitative analysis. Overall, we identified 21 cells that generated sufficiently robust responses to noradrenaline at 30 nM–10 μM with the threshold of 100–200 nM. Among them, 10 cells, which exhibited the same threshold of 150 nM, were taken for the analysis. To compare different experiments, responses of each particular cell recorded at variable agonist concentrations were normalized to a response to 1 μM noradrenaline and superimposed as shown in **Figure 2G**, where different symbols correspond to individual cells. Despite some data scattering, normalized cellular responses were localized in the narrow range of 0.8–1.2 (**Figure 2G**), clearly demonstrating that in all cases, the dose dependence was a step-like rather than gradual. Similar inference came from the analysis of 32 ATP-sensitive cells that showed quite robust responses to the nucleotide gradually applied at 0.5–50 μM. Of them, nine MSCs generated rather similar Ca^{2+} signals at gradually increasing ATP doses with the threshold of 1 μM (**Figure 2B**, **H**).

One more notable feature of MSC responses was that Ca^{2+} transients were markedly postponed relative to a moment of agonist application. The characteristic time of response delay (τ_d, **Figure 3A**) gradually decreased with noradrenaline and ATP concentration (**Figure 3B**, **C**). For instance, Ca^{2+} transients triggered by noradrenaline were retarded by 38–55 s at the threshold stimulation (**Figure 3A**, left response), whereas the delay was reduced to 17–26 s at the concentration of 1 μM and higher (**Figure 3A**, right response). The detailed assay of the dose-delay dependence was not carried out for the other agonists. Nevertheless, the comparison of MSCs responses obtained at low and saturated concentrations of adenosine, ADP, or UTP revealed a marked decrease in response delay as the agonist dose raised (**Figure 3D**). As discussed below, two distinct mechanisms are presumably responsible for specific dependencies of the magnitude and delay of MSC responses on agonist concentration.

3.2. Agonist transduction involves the phosphoinositide cascade and Ca^{2+}-induced Ca^{2+} release

In certain experiments, we analyzed coupling of adreno- and purinoreceptors to Ca^{2+} mobilization in the MSC cytoplasm. When MSCs were pretreated with U73122 (2–5 μM), a poorly reversible inhibitor of PLC, all assayed cells became completely nonresponsive to tested agonists, including noradrenaline (17 cells), ATP (39 cells), adenosine (11 cells), UTP (7 cells), and

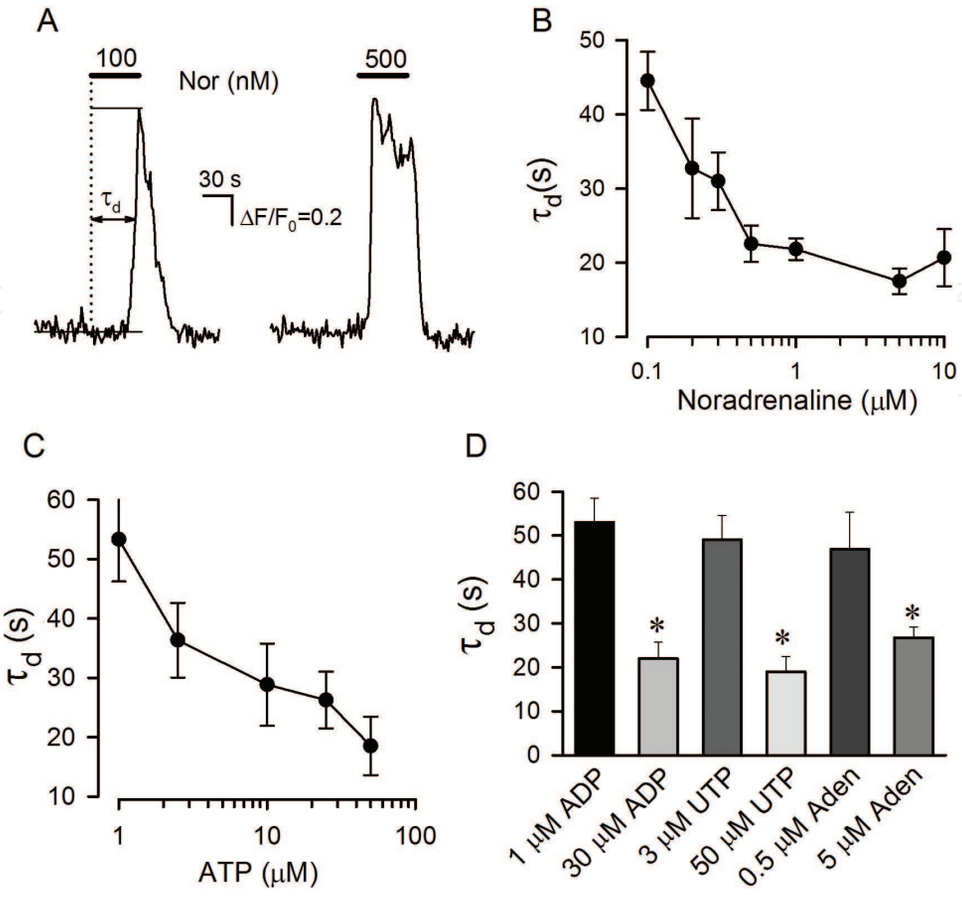

Figure 3. Dose dependence of agonist response delay. (A) Representative Ca^{2+} transients elicited by noradrenaline at 100 nM (threshold concentration) and 500 nM in the same cell. These noradrenaline responses were delayed relative to the moment of agonist application by 55 and 16 s, respectively. The characteristic time of the response delay (τ_d) was calculated as a time interval necessary for a Ca^{2+} transient to reach the half-magnitude. (B, C) Response lag versus noradrenaline (B) and ATP (C) concentration. The data were obtained from 10 adrenergic (**Figure 2A**, **G**) and 8 purinergic (**Figure 2B**, **H**) MSCs. (D) Delay of MSC responses to ADP (n = 16), UTP (n = 11), and adenosine (n = 21) at indicated concentrations. In (B–D), the data are presented as mean ± S.D.

ADP (5 cells) (**Figure 4A–C**, **G–I**). The inhibitory effect of U73122 on MSC responsiveness was apparently specific as the much less effective analog U73343 (2–5 μM) never canceled MSC responses to the nucleotides (**Figure 4A–C**, **G**, **H**). Moreover, the decrease of external Ca^{2+} from 2 mM to 260 nM weakly or negligibly affected Ca^{2+} transients elicited by ATP (26 cells), noradrenaline (31 cells), adenosine (7 cells), UTP (14 cells), and ADP (13 cells) (**Figure 4C**, **D**, **G–I**). Thus, the agonist-stimulated Ca^{2+} signaling in MSCs involved GPCRs that were basically coupled by the phosphoinositide cascade to Ca^{2+} release rather than to Ca^{2+} entry. Note also that the step-like dose dependence of ATP responses (**Figure 2B**, **H**) and their insignificant sensitivity to external Ca^{2+} (**Figure 4G**) indicated that P2X receptors could provide only a weak, if any, contribution to Ca^{2+} signaling triggered by ATP in the MSC cytoplasm.

Given the aforementioned effects of U73122 on MSC responses, there might be little doubt that the IP_3 receptor, a common effector downstream of PLC [30], was involved in transduction of assayed agonist. Expectedly, the IP_3 receptor blocker 2-APB (50 μM) suppressed Ca^{2+} signaling initiated by ATP (21 cells), noradrenaline (19 cells), adenosine (5 cells), ADP (9 cells), and UTP (10 cells) (**Figure 4D–I**)). In contrast, 50 μM ryanodine, a ryanodine receptor

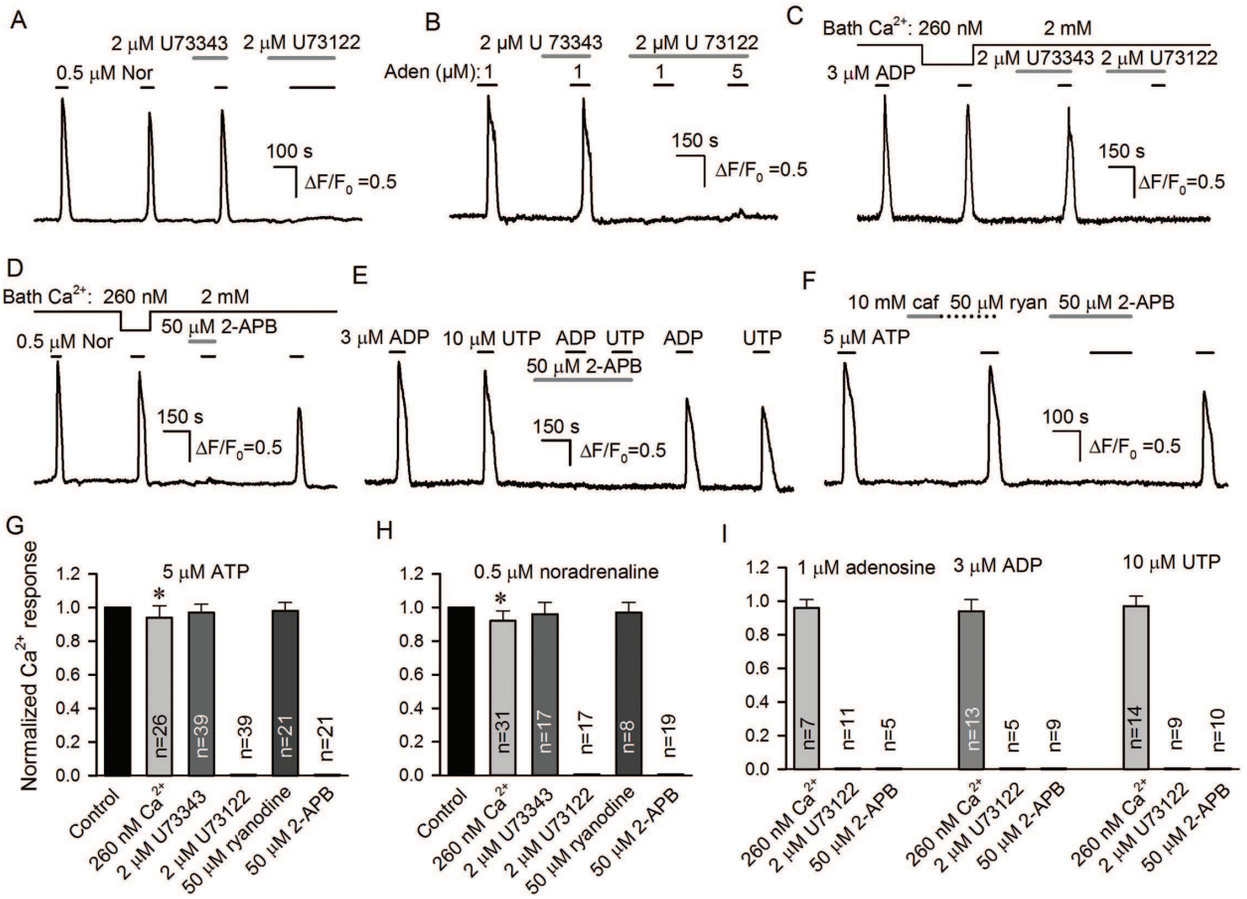

Figure 4. Involvement of the phosphoinositide cascade in agonist transduction. (A–C) PLC inhibitor U73122 (2 μM) suppressed MSC responsivity to different agonists, including 0.5 μM noradrenaline (A), 1 μM adenosine (B), and 3 μM ADP (C), while its much less effective analogue U73343 (2 μM) was ineffective in all cases. (C, D) Reduction of external Ca^{2+} from 2 mM to 260 nM weakly or negligibly affected Ca^{2+} responses to agonists, including 3 μM ADP and 0.5 μM noradrenaline. Extracellular Ca^{2+} was not completely removed because MSCs poorly tolerated prolonged exposure to a Ca^{2+}-free solution. (E, F) IP_3 receptor blocker 2-APB (50 μM) reversibly suppressed MSC responses, particularly, to 3 μM ADP, 10 μM UTP, and 5 μM ATP. (F) Caffeine and ryanodine, an agonist and antagonist of ryanodine receptors, respectively, negligibly affected cytosolic Ca^{2+} and ATP responsivity. (G–I) Summary of effects of indicated compounds and low Ca^{2+} on MSC responses to the tested agonists; n means the numbers of cells assayed in the particular case. The data are presented as mean ± S.D.; the asterisk indicates statistically significant difference (student t-test, $p < 0.05$).

antagonist, was ineffective in all cases (**Figure 4F–I**). These findings suggested a negligible role for ryanodine receptors in agonist transduction. Consistently, their agonist caffeine (10 mM) insignificantly affected cytosolic Ca^{2+} in ATP-responsive MSCs (7 cells; **Figure 4F**). It should be noted that 2-APB blocks not only IP_3 receptors but also a variety of Ca^{2+}-entry channels [31–33]. Given however that MSC responsiveness to P2Y agonists insignificantly depended on external Ca^{2+} and therefore on Ca^{2+} influx (**Figure 4G–I**), we inferred that 2-APB exerted the inhibitory action mainly by targeting IP_3 receptors.

The monotonic and gradual dependence of cellular responses on agonist concentration has been reported for a variety of cellular systems, including those that employ GPCRs coupling to Ca^{2+} mobilization [34–36]. In contrast, Ca^{2+} responses were generated by MSCs in an "all-or-nothing" manner (**Figure 2**). This step-like dose dependence of response magnitude is poorly explicable and apparently inconsistent with the gradual relation between response delay and agonist concentration (**Figure 3**) if agonist transduction involves solely PLC-dependent

production of an IP_3 burst and proportional Ca^{2+} release via IP_3 receptors. To address this problem, we assumed that the agonist transduction occurred in two separated consecutive steps. Initially, an agonist produced a Ca^{2+} signal most likely being small, local, and gradually dependent on stimulus intensity. When exceeding the threshold, this local and poorly resolved Ca^{2+} signal pushed massive Ca^{2+}-induced Ca^{2+} release (CICR) [37–40] to accomplish transduction with a large and global Ca^{2+} signal. By involving the trigger-like mechanism CICR, a cell generates Ca^{2+} responses of virtually universal shape and magnitude at different agonist concentrations above the threshold (**Figure 2**). Rising with agonist proportionally, the initial gradual Ca^{2+} signal reached a CICR threshold for the time that should have shortened with agonist concentration, thus underlying the gradual dose-delay dependence observed (**Figure 3B**, **C**).

To clarify functionality of the CICR mechanism in MSCs and its contribution to agonist responses, we used Ca^{2+} uncaging that allowed for generating as fast and intensive cytosolic Ca^{2+} bursts as necessary for initiating the CICR process. In designated experiments, MSCs were loaded with both Fluo-4 and NP-EGTA. The last is photolabile Ca^{2+} chelator with high affinity to Ca^{2+} (Kd ~ 10^{-7} M), so that in a resting cell (~100 nm free Ca^{2+}), nearly half NP-EGTA molecules are bound to Ca^{2+} ions. The absorption of ultraviolet (UV) light by NP-EGTA disrupts the coordination sphere responsible for Ca^{2+} binding, thus liberating Ca^{2+}ions and producing a step-like increase in cytosolic Ca^{2+} [41]. Because a UV laser we employed for uncaging was in fact a biharmonic light source emitting at 351 and 527 nm, a light stimulus caused an optical artifact that was seen as a marked overshoot in a recording trace of cell fluorescence acquired at 535 ± 25 nm.

In this series, caged Ca^{2+} was released by moderate UV pulses during several seconds to somehow simulate the suggested Ca^{2+} signal initially produced by agonists in the MSC cytoplasm. As illustrated in **Figure 5A**, light stimuli triggered in adrenergic MSCs (n = 33) two fundamentally different types of Ca^{2+} responses. The relatively short, 2-s in the given case, UV pulse produced an optical artifact that was followed by a small Ca^{2+} jump without evident delay (**Figure 5A**, left panel, response 1 and right panel, thick line). This Ca^{2+} signal exhibited exponential relaxation presumably mediated by Ca^{2+} pumps. The sequential 4-s and 6-s UV flashes elicited biphasic Ca^{2+} transients of nonproportional magnitudes (**Figure 5A**, left panel). Indeed, compared to a 2-s UV pulse, one could expect 4- and 6-s light stimuli to liberate nearly twice and three times more Ca^{2+} ions, respectively. Meanwhile, 4-, 6-, and 8-s flashes usually triggered the similar Ca^{2+} transients that exceeded a response to a 2-s pulse by an order of magnitude (**Figure 5A**, left panel). None of the known Ca^{2+}-dependent mechanisms but CICR could amplify and shape an initial Ca^{2+} signal produced by NP-EGTA photolysis in such a way (**Figure 5A**, right panel, response 1 vs. response 2). In addition, the representative cell (**Figure 5A**, left panel) was insensitive to 50 nM noradrenaline but similarly responded to the agonist at 0.5 and 1 μM concentrations. Similar results were obtained with other eight MSCs that tolerated prolonged serial stimulation with both UV and noradrenaline. Note that biphasic cell responses to light and noradrenaline were quite similar by shape and magnitude (**Figure 5A**, right panel, thin line 2 and circled line 3). Interestingly, light responses exhibited the delay that shortened with UV pulse duration (**Figure 5**, left panel). Similar experiments were performed with purinergic MSCs (n = 23) and basically identical results were obtained (**Figure 5B**). These findings support the idea that the delay of agonist responses (**Figure 3**) could be determined by the initial gradual Ca^{2+} signal.

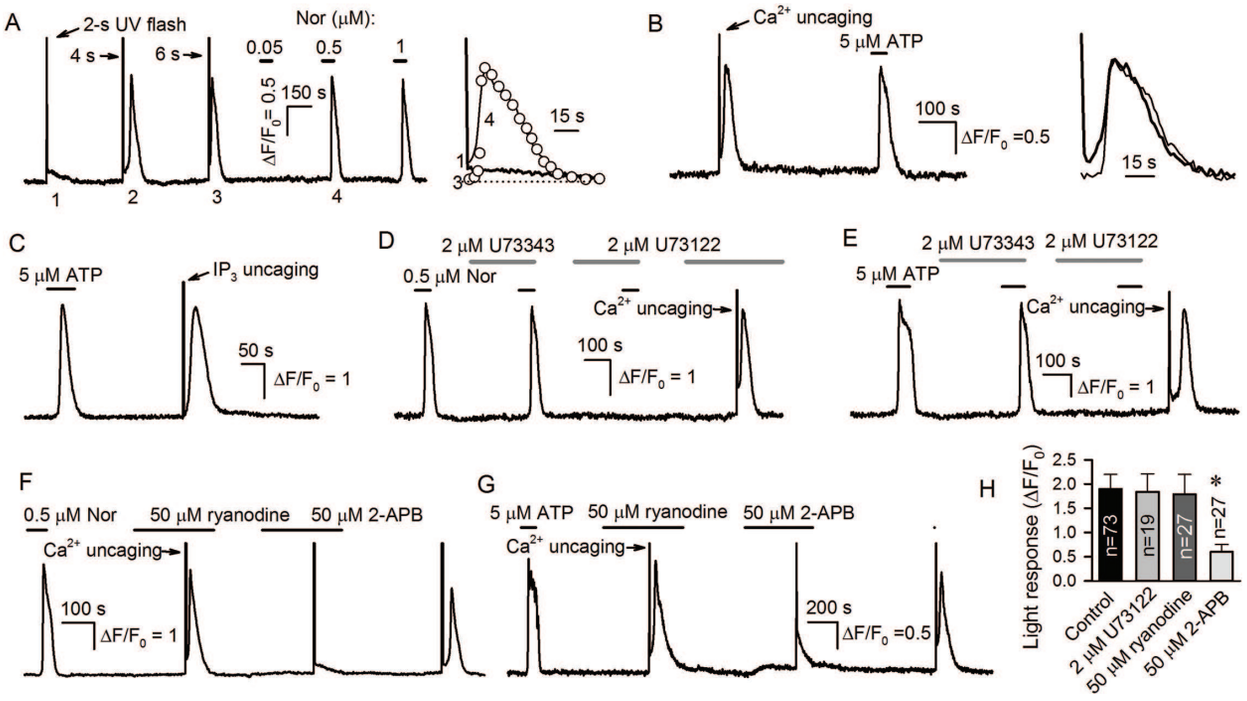

Figure 5. Evidence for Ca^{2+}-induced Ca^{2+} release in MSCs. (A) Left panel—Ca^{2+} transients resulted from Ca^{2+} uncaging in a NP-EGTA loaded cell by UV flashes of varied durations and Ca^{2+} responses to noradrenaline at the indicated concentrations. Right panel—The superimposition of the responses numbered in (A) as 1 (thick line), 3 (circles), and 4 (thin line). (B) Left panel—Cellular responses to Ca^{2+} uncaging produced by a 4-s UV flash and to 5 μM ATP. Right panel—The superimposition of the light (thick line) and ATP (thin line) responses shown in the left panel. (C) ATP (5 μM) and uncaging of IP_3 by a 2-s UV flash elicited similar responses in a cell loaded with caged-Ins(145)P3/PM. (D, E) PLC inhibitor U73122 (2 μM) dumped MSC responsiveness to 0.5 μM noradrenaline (D) and 5 μM ATP (E) but did not prevent agonist response-like Ca^{2+} transients resulted from Ca^{2+} uncaging by 4-s UV flashes. (F, G) 2-APB (50 μM) completely abolished biphasic agonist-like responses to Ca^{2+} uncaging by 4-s UV flashes, while 50 μM ryanodine was ineffective. In the experiments presented in (A–G), emission of a UV laser was weakened by the factor 10, so that Ca^{2+} uncaging should have lasted for 4 s to liberate as many Ca^{2+} ions as necessary for stimulating CICR. This gradual release of caged Ca^{2+} somewhat slowed the rising phase of a biphasic Ca^{2+} transient produced by CICR, thereby making a lag between a UV flash and a light response clearly visible. (H) Summary of effects of 2 μM U73122, 50 μM ryanodine, or 50 μM 2-APB on Ca^{2+} transients elicited by 4-s UV flashes. The data are presented as mean ± SD; the asterisk indicates statistically significant difference (student t-test, $p < 0.05$).

Similar to Ca^{2+} uncaging (**Figure 5A**), uncaging of IP_3 produced agonist-like responses in purinergic (n = 14) and adrenergic (n = 6) MSCs (**Figure 5C**). It was therefore possible that Ca^{2+} uncaging could simulate agonist-like responses by stimulating Ca^{2+}-dependent PLC [42–44], which quickly generated a sufficient IP_3 burst, thereby enhancing activity of IP_3 receptors and triggering CICR. To verify this possibility, several adrenergic (n = 12) and purinergic (n = 7) MSCs loaded with NP-EGTA were subjected to Ca^{2+} uncaging in the presence of U73122. Although this PLC inhibitor expectedly rendered MSCs nonresponsive to the agonists, the cells normally responded to UV flashes (**Figure 5D**, **E**). The ineffectiveness of U73122 (**Figure 5D**, **E**, **H**) provided strong evidence that PLC activation was not obligatory for generating light responses, thereby demonstrating that CICR initiated by UV flashes was directly stimulated by Ca^{2+} ions liberated from NP-EGTA.

Reportedly, ryanodine and inositol 1,4,5-trisphosphate (IP_3) receptors, Ca^{2+}-gated Ca^{2+} release channels operating in the endo/sarcoplasmic reticulum, are exclusively responsible for CICR

in apparently all cells [39, 42, 44]. To evaluate a relative contribution of IP_3 and ryanodine receptors to CICR in MSCs, we examined effects of their antagonists on Ca^{2+} signals associated with Ca^{2+} uncaging. While 50 μM ryanodine was ineffective, 50 μM 2-APB dramatically and reversibly changed a shape and magnitude of UV responses in adrenergic (n = 16) and purinergic (n = 11) MSCs (**Figure 5F–H**). In the presence of 50 μM ryanodine, Ca^{2+} uncaging elicited agonist-like biphasic Ca^{2+} responses that were delayed relative to stimulatory UV flashes (**Figure 5F**, **G**, 2nd responses). Thus, despite the inhibition of ryanodine receptors, Ca^{2+} uncaging was still capable of stimulating robust CICR in MSCs responsive to the agonists. With 50 μM 2-APB in the bath, a UV pulse entailed a brief Ca^{2+} jump that relaxed monotonically and was smaller by the factor 3–4 (**Figure 5F**, **G**, 3rd responses; **Figure 5H**). This indicated that Ca^{2+} uncaging failed to initiate CICR with inhibited IP_3 receptors. Moreover, when 2-APB was removed to restore activity of IP_3 receptors, a UV flash triggered a biphasic Ca^{2+} transient again (**Figure 5F**, **G**, 4th responses). These observations indicated that basically IP_3 receptors were responsible for CICR in adrenergic and purinergic MSCs.

3.3. Adrenoreceptor subtypes involved in Ca^{2+} signaling

Nine human genes encode adrenoreceptors, including α_{1A}, α_{1B}, α_{1D}, α_{2A}, α_{2B}, α_{2C}, β_1, β_2, and β_3 isoforms [45]. Previously, we demonstrated that transcripts for α_{1B}-, α_{2A}-, and β_2-adrenoreceptors were invariably present in total MSC preparations [24]. Given that both α_1- and α_2-adrenoreceptors are routinely coupled to PLC and Ca^{2+} mobilization in different cells [21, 22], either or both of these isoforms might be responsible for Ca^{2+} transients generated by MSCs in response to noradrenaline (**Figure 2A**). In contrast, β_2-adrenoreceptors, which generally involve adenylyl cyclase as a downstream effector [23], could not be an essential contributor to Ca^{2+} signaling in adrenergic MSCs.

To uncover a role of the particular isoform, we performed recordings using agonists and antagonists specific for α_1- or α_2-adrenoreceptors. Overall, 35 noradrenaline-responsive cells were treated with phenylephrine/cirazoline and prazosin (α_1-agonists and antagonist, respectively) as well as with guanabenz/B-HT 933 and yohimbine (α_2-agonists and antagonist, respectively). Most of them (29 cells, 83%) were irresponsive to phenylephrine (1–10 μM), and their noradrenaline responses were not inhibited by 10 μM prazosin. In contrast, guanabenz (10–50 μM) and B-HT 933 (10 μM) were quite effective (**Figure 6A**). In particular, 50 μM guanabenz stimulated Ca^{2+} signaling in all noradrenaline-responsive MSCs (**Figure 6A–C**). Consistently, 2 μM yohimbine dumped cellular responses to noradrenaline and guanabenz (**Figure 6A**). Six cells (17%) were sensitive to both 10 μM phenylephrine and 50 μM guanabenz (**Figure 6B**, **C**). These findings indicate that the α_2-subtype, evidently α_{2A}, predominantly mediates Ca^{2+} signaling initiated by noradrenaline in MSCs, although in a minor MSC subpopulation, both α_1- and α_2-isoforms could be involved in adrenergic transduction.

3.4. Effects of isoform-specific agonists and antagonists of P2Y receptors

In mammalians, the P2Y subgroup includes eight GPCRs ($P2Y_{1,2,4,6,11–14}$) that exhibit certain specificities to nucleotides, depending on species [18, 46]. The expression of purinoreceptors in MSCs was analyzed previously, and transcripts for multiple P2Y receptors were detected,

namely, $P2Y_1$, $P2Y_2$, $P2Y_4$, $P2Y_6$, $P2Y_{11}$, $P2Y_{13}$, and $P2Y_{14}$, while $P2Y_{12}$ transcripts were not detected in total MSC preparations [47]. Although this P2Y array is sufficient to account for MSC capability to detect ATP, ADP, and UTP, it was impossible to evaluate a contribution of a particular P2Y isoform based on MSC responses to these natural P2Y agonists (**Figure 2B**, **E**, **F**). To address this issue, we used isoform-specific P2Y agonists and antagonists.

The human P2Y family contains two ATP receptors, including specialized $P2Y_{11}$ and also $P2Y_2$ that recognizes both UTP and ATP as full equipotent agonists [18]. Although also known as a partial $P2Y_1$ agonist, ATP was hardly capable of stimulating $P2Y_1$-signaling in MSCs at low micromolar concentrations due to much lower efficacy than ADP [48]. We tried to evaluate a contribution of $P2Y_{11}$ and $P2Y_2$ to MSC responsiveness to ATP. Among 181 MSCs assayed in this series, 169 cells (93%) became nonresponsive to ATP (3 μM) in the presence of 30 μM NF 340, a specific $P2Y_{11}$ antagonist. These NF 340-sensitive cells did not respond to the $P2Y_2$

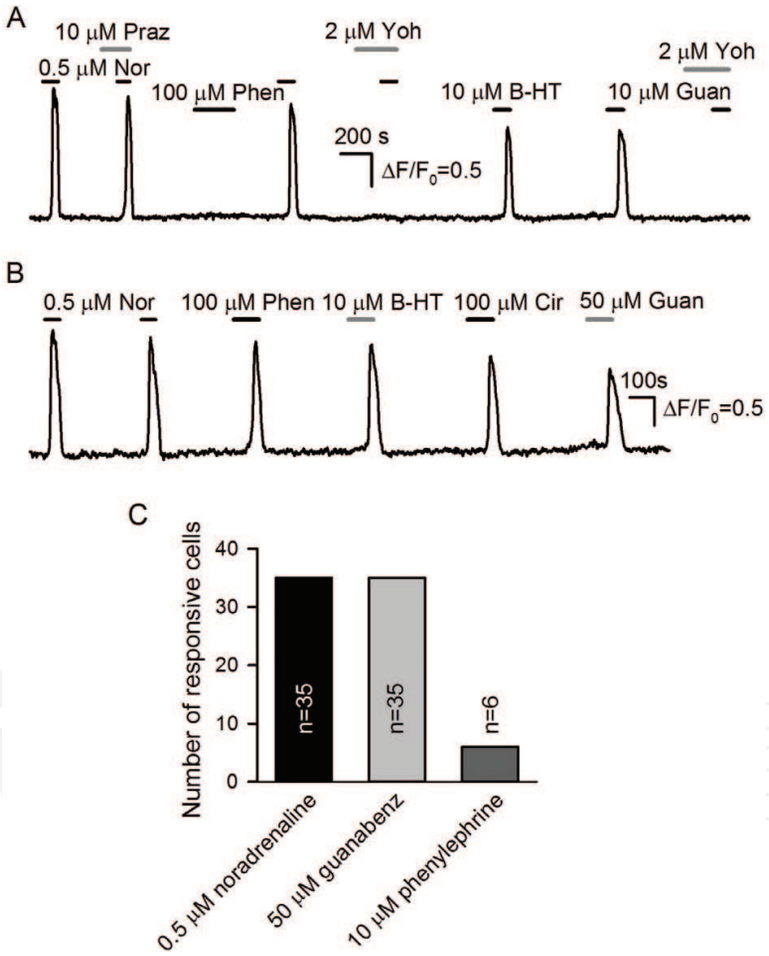

Figure 6. Sensitivity of MSCs to adrenergic agonists and antagonists. (A) In most (83%) of noradrenaline-sensitive MSCs, α2-receptor agonists B-HT 933 and guanabenz stimulated Ca^{2+} signaling in contrast to the α1-receptor agonists phenylephrine and cirazoline that were ineffective. Consistently, Ca^{2+} signaling stimulated in such cells by noradrenaline and guanabenz was canceled in the presence of the α2 antagonist yohimbine, while the α1 antagonist prazosin was ineffective. (B) Small subpopulation (17%) of noradrenaline-sensitive cells responded to both α2 and α1 agonists. (C) Responsiveness of 35 MSCs sequentially stimulated by 0.5 μM noradrenaline, 50 μM guanabenz, and 10 μM phenylephrine.

agonist MRS 2768 (10 μM) (**Figure 7A**, cell 1 and **Figure 7B**). In a subpopulation of rare MSCs (12 cells) that were capable of generating Ca^{2+} transients on 3 μM ATP in the presence of NF 340, 11 cells also responded to 10 μM MRS 2768 (**Figure 7A**, cell 2 and **Figure 7B**). Thus, MSCs that were insensitive to NF 340 presumably employed $P2Y_2$ or both $P2Y_2$ and $P2Y_{11}$ to detect ATP.

While the $P2Y_{11}$ antagonist was highly effective (**Figure 7A**, **B**), most ATP-sensitive MSCs were surprisingly nonresponsive to NF 546 (10 μM), the specific $P2Y_{11}$ agonist reported to be even more effective than ATP [49]. Among 127 cells that responded to 3 μM ATP, 10 μM NF 546 stimulated Ca^{2+} signaling solely in 9 cells (7%; **Figure 7C**, **D**). At the moment, we cannot provide any valid explanation for very low efficacy of NF-546 relative to ATP (**Figure 7D**). Perhaps, this synthetic ligand is a biased agonist that enables coupling of $P2Y_{11}$ to the phosphoinositide cascade by involving only a certain G-protein type, which is absent or relatively less abundant in most of the MSCs.

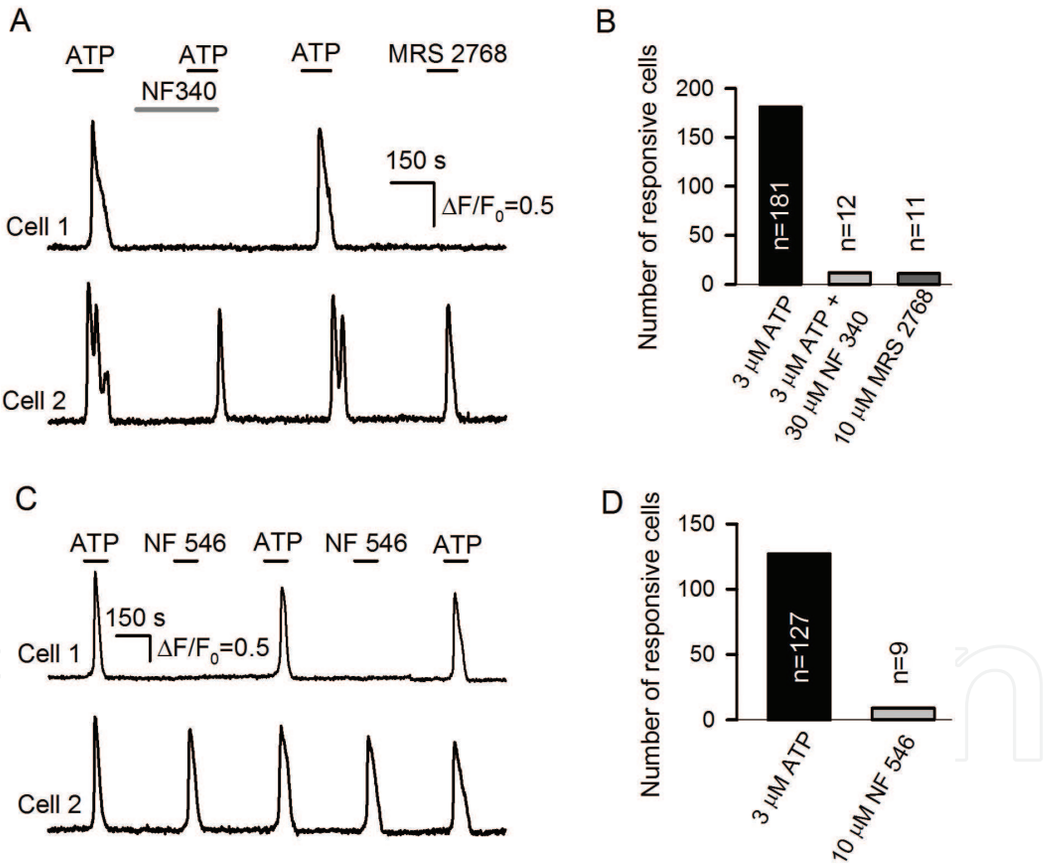

Figure 7. Sensitivity of MSCs to agonists and antagonists of $P2Y_2$ and $P2Y_{11}$ receptors. (A) Representative responses of two concurrently assayed cells to ATP (3 μM) and to the $P2Y_2$ agonist MRS 2768 (10 μM). The great majority (93%) of ATP-sensitive MSCs were rendered nonresponsive by 30 μM NF 340, a $P2Y_{11}$ antagonist, and such cells never responded to 10 μM MRS 2768 (Cell 1). Uncommon cells that remained sensitive to ATP in the presence of 30 μM NF 340 responded to 10 μM MRS 2768 as well (Cell 2). (B) Responsiveness of 181 MSCs to 3 μM ATP and 10 μM MRS 2768 assayed in control and in the presence of NF 340. (C) Representative concurrent recordings from an ordinary cell insensitive to 10 μM NF 546 (Cell 1) and from an occasional cell responsive to this specific $P2Y_{11}$ agonist (n = 127; Cell 2). (D) Responsiveness of 127 MSCs to 3 μM ATP and 10 μM NF 546.

UTP is a full agonist for $P2Y_2$ and $P2Y_4$ that were identified in MSCs at the population level [47]. It therefore was unclear whether a particular cell employs either or both of these P2Y receptors for monitoring extracellular UTP. We analyzed the sensitivity of 95 UTP-responsive MSCs to MRS 2768 and MRS 4062, specific agonists of $P2Y_2$ and $P2Y_4$ receptors, respectively. Consistently with the analysis of ATP-responsive cells (**Figure 7B**), we found only 9 (9.5%) of 95 UTP-sensitive cells to react to 10 μM MRS 2768 (**Figure 8A**, cell 3 and **Figure 8B**).

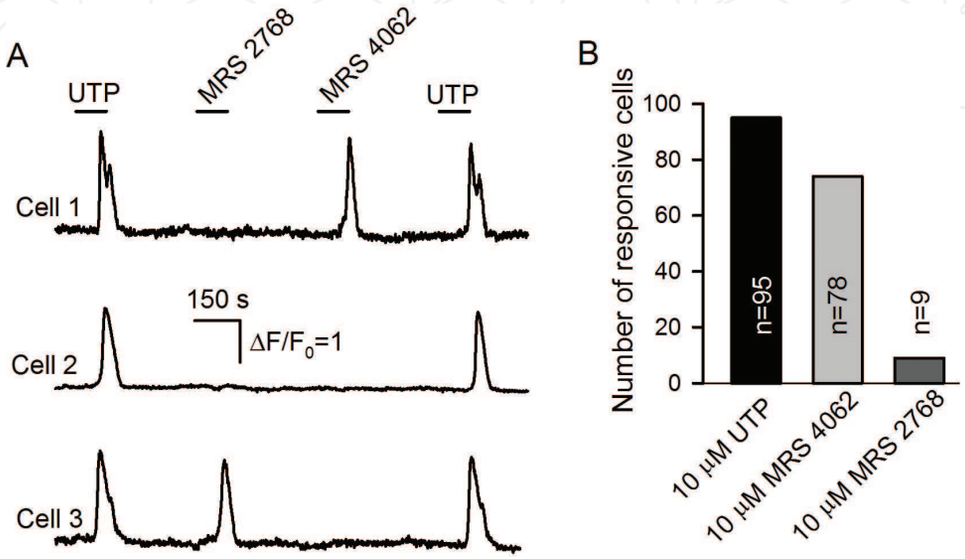

Figure 8. Sensitivity of UTP-responsive MSCs to $P2Y_2$ and $P2Y_4$ agonists. (A) Representative recordings from purinergic MSCs stimulated by UTP (10 μM), MRS 2768 (10 μM), and the agonists of $P2Y_4$ receptor MRS 4062 (10 μM), in series. (B) Responsiveness of UTP-sensitive MSCs (n = 95) to MRS 2768 and MRS 4062.

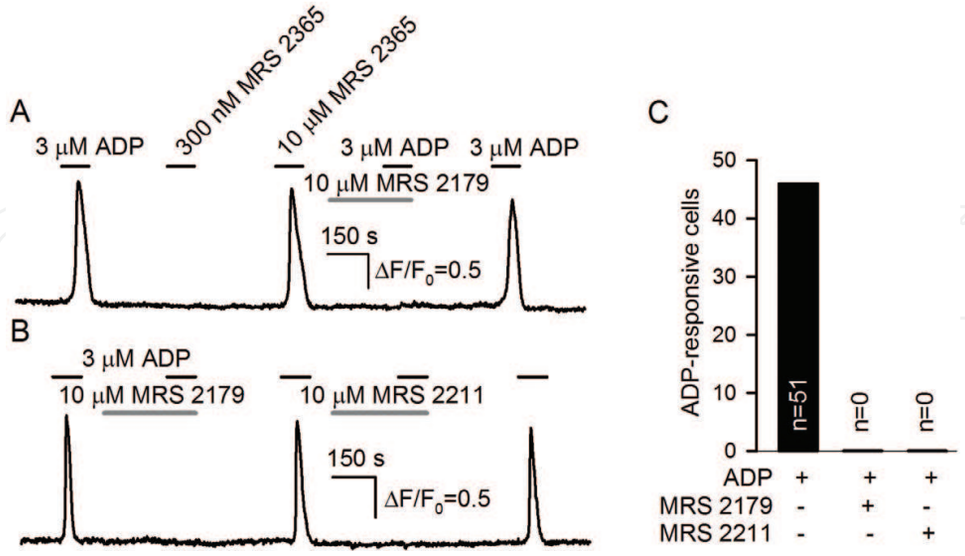

Figure 9. Contribution of $P2Y_1$ and $P2Y_{13}$ to ADP responsiveness. (A) Representative MSC responses to 3 μM ADP and to the $P2Y_1$ agonist MRS 2365 applied at 300 nM and 10 μM. All cells treated with 10 μM MRS 2179 (n = 65) became nonresponsive to 3 μM ADP. (B) When applied alone at 10 μM, antagonists of $P2Y_1$ (MRS 2179) and $P2Y_{13}$ (MRS 2211) inhibited responses of MSCs to 3 μM ADP (46 cells). (C) Summary of responses of 51 MSCs to 3 μM ADP in control and in the presence of MRS 2179 or MRS 2211.

In contrast, 78 cells (82%) responded to 10 μM MRS 4062 (**Figure 7A**, cell 1 and **Figure 7B**). These findings suggested that predominantly $P2Y_4$ was responsible for Ca^{2+} signaling evoked in MSCs by UTP, while $P2Y_2$ was either expressed in a very small subpopulation of $P2Y_4$-negative cells or not coupled to Ca^{2+} mobilization in a great majority of $P2Y_4$-positive cells.

Extracellular ADP is detected by cells with $P2Y_1$, $P2Y_{12}$, and $P2Y_{13}$. The analysis of ADP responsiveness was performed on 102 MSCs sensitive to 3 μM ADP (**Figure 8A**) that might be recognized by $P2Y_1$ and/or $P2Y_{13}$ receptors, given that $P2Y_{12}$ transcripts were not found in MSCs. To evaluate a role of the $P2Y_1$, 65 of 103 ADP-sensitive MSCs were treated with MRS 2365, a highly potent and selective $P2Y_1$ agonist that displays no activity at $P2Y_{12}$ and $P2Y_{13}$ at submicromolar concentrations [50]. MRS 2365 was ineffective at 100–300 nM but triggered Ca^{2+} signaling in 16 (25%) of 65 MSCs at 10 μM (**Figure 9A**). Because MRS 2365 specifically stimulates $P2Y_1$ with EC_{50} ~ 1 nM [50], this agonist might bring about a nonspecific action at 10 μM. On the other hand, MRS 2179 (10 μM), a $P2Y_1$ antagonist with IC_{50} = 0.15 μM [49], inhibited ADP responses in all MRS 2365-treated MSCs (65 cells; **Figure 9A**). Given that other P2Y receptors were hardly inhibited by 10 μM MRS 2179 [49], the observed effects of the specific agonist and antagonist of the $P2Y_1$ receptor were rather inconsistent. To reconcile these contradictory findings, we considered the possibility that both $P2Y_1$ and $P2Y_{13}$ should have been activated by ADP concurrently to mobilize Ca^{2+} in MSCs. If so, nanomolar MRS 2365 was ineffective, activating solely $P2Y_1$, while 10 μM MRS 2365 stimulated activity of both $P2Y_1$ and $P2Y_{13}$ [50], thus triggering Ca^{2+} signaling in MSCs. This concept predicted that MSCs would be unable to respond to ADP if either $P2Y_1$ or $P2Y_{13}$ was inhibited. In line with this idea, we assayed sensitivity of 51 ADP-responsive MSCs to both MRS 2179 (10 μM) and MRS 2211 (10 μM), a $P2Y_{13}$ antagonist. It turned out that either of these compounds rendered each of 51 assayed cells nonresponsive to ADP (**Figure 9B**, **C**). Altogether, our findings (**Figure 9A–C**) indicated that only those MSCs, which functionally expressed both $P2Y_1$ and $P2Y_{13}$ receptors, were capable of generating robust Ca^{2+} responses to ADP.

4. Discussion

Virtually in all cell types, extracellular cues can mobilize intracellular Ca^{2+} to regulate a variety of diverse cellular functions, such as fertilization, proliferation, secretion, metabolism, gene expression, mobility, and muscle contraction. How can the Ca^{2+} ion, a chemically simple substance, control so many different physiological processes? The plausible explanation comes from the versatility of Ca^{2+} signaling mechanisms that can mediate Ca^{2+} signals with variable kinetics, amplitude, duration, and spatial patterning, depending on cellular context and stimulation [30, 37, 42].

Transduction of multiple agonists involves GPCRs coupled to $PLC\beta_{1–4}$ isoforms that hydrolyze the precursor lipid phosphatidylinositol 4,5-bisphosphate to produce two second messengers, IP_3 and diacylglycerol. The primary mode of action of IP_3 is to bind to IP_3 receptors and release Ca^{2+} from the endoplasmic reticulum (ER) [30, 51, 52]. Three different isoforms of the IP_3 receptor have been identified (IP_3R1, IP_3R2, and IP_3R3) and shown to serve as a tetrameric IP_3-gated Ca^{2+} channel [30, 51–53]. IP_3R1, IP_3R2, and IP_3R3 are distinct by physiological

properties, thus allowing cells to generate specific Ca^{2+} signals with different spatial and temporal characteristics to control diverse cellular functions [30, 52]. In addition to IP_3, Ca^{2+} is the primary coregulator of IP_3 receptors [30, 51, 52, 54]. The full activation of the IP_3 receptor occurs when IP_3 has occupied the IP_3-binding domains on all four subunits [55]. This is associated with a conformational change, which sensitizes the Ca^{2+}-binding site. The binding of cytosolic Ca^{2+} to this site markedly increases the open probability of the IP_3 receptor channel [54], so that Ca^{2+} ions released from the ER can additionally stimulate activity of IP_3 receptors. This positive feedback mediates CICR. Meanwhile, the action of cytosolic Ca^{2+} is bimodal: stimulating IP_3 receptors at low levels, Ca^{2+} becomes inhibitory above 300 nm [54]. This multimodal control of the IP_3 receptor by IP_3 and Ca^{2+} is central to various aspects of intracellular Ca^{2+} signaling [30, 52].

In the present work, we studied MSCs from the human adipose tissue and examined intracellular Ca^{2+} signaling initiated by certain GPCR agonists, including adenosine, ATP, noradrenaline, and some others. Although all first messengers tested here were effective, only a relatively small MSC group responded to a particular agonist. These specifically responsive cell subpopulations overlapped weakly or negligibly, depending on agonists (**Figure 1**). This finding is hardly surprising in light of a widely accepted idea that a MSC population from different sources represents a heterogeneous mixture of diverse cells, including multipotent and more committed progenitor cells [1, 3, 56, 57]. Yet, cultured MSCs are not synchronized and dwell in different phases of the cell cycle. It therefore might be expected that divergent intracellular signaling is inherent in a MSC population containing both proliferating and quiescent cells. The aforementioned factors could underlie intrinsic heterogeneity of a MSC population discussed previously [56, 57]. It also should be mentioned that most of assayed MSCs were found by us nonresponsive to a particular agonist solely in terms of Ca^{2+} signaling that necessitated coupling of appropriate GPCRs to Ca^{2+} mobilization. Meanwhile, many GPCR isoforms are in fact promiscuous in that they may be coupled to a variety of downstream signaling pathways, depending on G-proteins involved. For instance, the $P2Y_{1,2,4,6,11}$ subtypes of purinoreceptors are canonically coupled by G_q/G_{11} to the phosphoinositide cascade and Ca^{2+} mobilization, whereas $P2Y_{12,13,14}$ control cAMP production by inhibiting adenylyl cyclase through G_i/G_o. The unique capability of $P2Y_{11}$ is to stimulate G_s [18]. In addition, apart from ubiquitous coupling to PLC and adenylyl cyclase, P2Y receptors can also engage effectors such as MAP, PI3, Akt, and PKC kinases; small G-proteins; NO synthase; transactivation of growth factor receptors; and some others [26–29]. Hence, a fraction of MSCs sensitive to a given agonist might be in fact much more abundant than that evaluated by Ca^{2+} imaging (**Figure 1B**, **C**), because the tested compounds could stimulate not only Ca^{2+} mobilization but also other signaling events.

The agonist-dependent Ca^{2+} signaling in MSCs was mostly detailed by us for noradrenaline and certain nucleotides. By using subtype-specific agonists and antagonists, it was shown that mainly a_2-adrenoreceptors mediated Ca^{2+} mobilization triggered by noradrenaline in adrenergic MSCs (**Figure 6**). In purinergic MSCs, presumably $P2Y_{11}$ serves as a primary ATP receptor (**Figure 7**), UTP responsiveness is largely mediated by $P2Y_4$ (**Figure 8**), while both $P2Y_1$ and $P2Y_{13}$ are involved in detecting ADP (**Figure 9**). The responsivity of MSCs to noradrenaline and ATP and apparently to adenosine, ADP, and UTP exhibited a peculiar dose dependence:

undetectably affecting intracellular Ca^{2+} below the cut-off concentration, a particular agonist initiated Ca^{2+} transients that were large and quite similarly shaped at all doses above the threshold (**Figure 2**). In contrast to this step-like dose-response curve, the dependence of response delay on agonist concentration was gradual (**Figure 3**). The inhibitory analysis and Ca^{2+} uncaging approach showed that agonist transduction universally involved the classical phosphoinositide cascade and CICR mechanism (**Figures 4** and **5**) that employed IP_3 receptors rather than ryanodine receptors (**Figures 4E**, **F** and **5F**, **G**).

To reconcile the "all-or-nothing" dose-response curve and gradual dose-delay dependence, we surmised that agonist-evoked Ca^{2+} signaling in MSCs includes two different but coupled stages. Primarily, agonists stimulate IP_3 production, activation of IP_3 receptors, and generation of an initial, presumably local and gradual Ca^{2+} signal. Next, this local Ca^{2+} signal stimulates CICR that produces a global Ca^{2+} signal. Some evidence suggests that the Ca^{2+} store responsible for the initial Ca^{2+} signal may be physically separated from the Ca^{2+} store that provides CICR. Indeed, when cells were overloaded with NP-EGTA due to the twofold excess of NP-EGTA-AM concentration compared to the standard loading protocol (see Methods), a MSC population became poorly sensitive to ATP. However, several UV flashes usually rendered MSC responsive (**Figure 10**). Presumably, overloading with NP-EGTA excessively increased the Ca^{2+}-buffering capacity of the cell cytoplasm, thereby significantly diminishing the initial agonist-induced Ca^{2+} signal and its speed. The photodistraction of NP-EGTA decreased exogenous Ca^{2+} buffer to a physiologically more relevant level, thus recovering MSC responsiveness to ATP. Note that in line with multiple reports, relatively slow Ca^{2+} buffer EGTA is unable to cancel Ca^{2+}-dependent processes mediated by local intracellular Ca^{2+} signals. For instance, 1 mM EGTA does not prevent activation of Ca^{2+}-gated BK channels by Ca^{2+} transients originated by both Ca^{2+} influx via voltage-gated Ca^{2+} channels and Ca^{2+} release stimulated by muscarine [58]. By analogy and based on the observation that Ca^{2+} uncaging was still capable of triggering CICR in MSCs overloaded with NP-EGTA (**Figure 10**), we suggested that NP-EGTA, slow Ca^{2+} buffer [59], could hardly repeal stimulation of IP_3 receptors by Ca^{2+} ions released through this IP_3-gated conduit. If so, the Ca^{2+} store and IP_3 receptor pool mediating CICR should be spatially separated from agonist-dependent machinery that

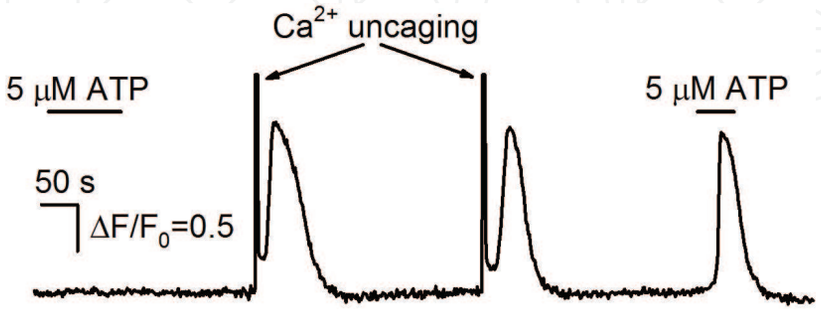

Figure 10. MSCs overloaded with NP-EGTA became nonresponsive to agonists. In this particular experiment, 76 cells, which have been pre-incubated with 4 μM Fluo-4-AM and 8 μM instead of 4 μM NP-EGTA-AM, were simultaneously assayed. None of these cells generated Ca^{2+} responses to the first application of 5 μM ATP. As exemplified by the presented fluorescence trace, two sequential Ca^{2+} uncaging by 4-s UV flashes rendered 7 of 76 cells sensitive to 5 μM ATP. The same phenomenon was observed in two more similar experiments.

generates an initial, local, and gradual Ca^{2+} signal. Otherwise, it is difficult to explain why in cells overloaded with NP-EGTA, agonist responses disappeared contrary to light responses associated with Ca^{2+} uncaging (**Figure 10**).

5. Conclusion

Note in conclusion that the specific features of agonist responses, including kinetics and magnitude, all-or-nothing behavior and gradual dose-response delay were correctly reproduced by Ca^{2+} signals elicited by Ca^{2+} uncaging (**Figure 5**). This supports the idea that agonist-evoked Ca^{2+} signaling in MSCs includes two different but coupled stages. Initially, agonists stimulate coupling of suitable GPCRs via appropriate G-proteins to PLC, thus triggering IP_3 production, activation of IP_3 receptors (IP_3R_{grad}) followed by the release of Ca^{2+} ions from Ca^{2+} store. This machinery generates an initial, presumably local and gradual Ca^{2+} signal (**Figure 11**). When exceeding the threshold, this local Ca^{2+} signal stimulates CICR that is mediated by IP_3 receptors (IP_3R_{CICR}) presumably located in another, spatially separated Ca^{2+} store. By involving the trigger-like mechanism CICR, a cell generates Ca^{2+} responses of virtually universal shape and magnitude at different agonist concentrations above the

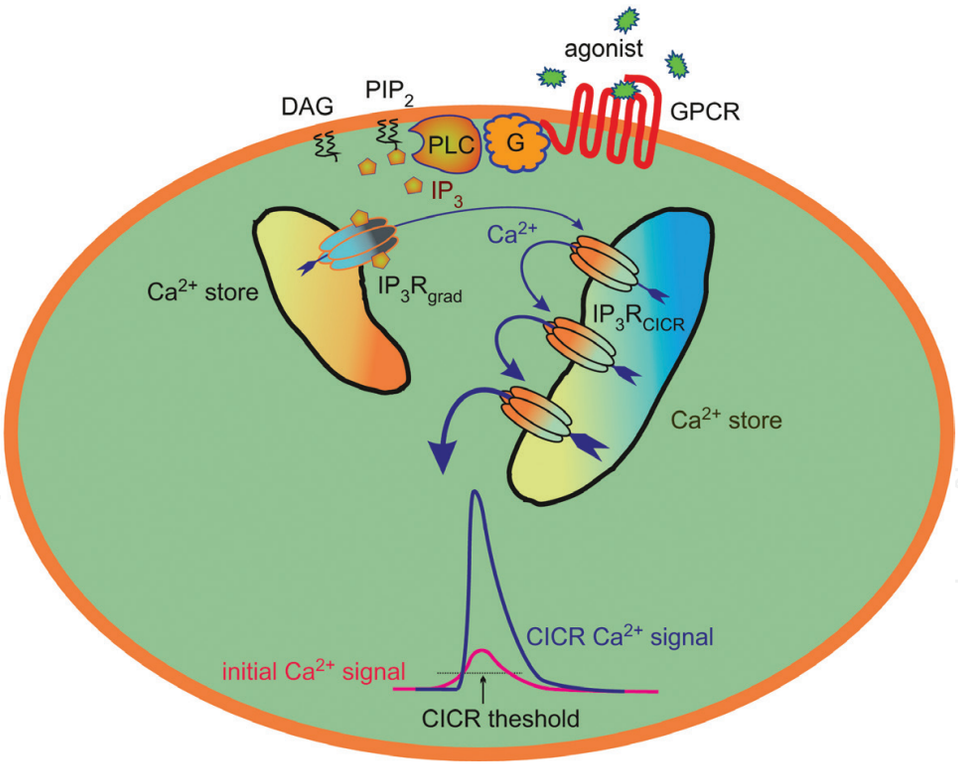

Figure 11. Working model of agonist transduction in MSCs. The binding of agonists to GPCRs stimulates PLC-dependent hydrolysis of PIP_2 to DAG and IP_3. The consequent activation of IP_3 receptors (IP_3R_{grad}) mediates Ca^{2+} release from related Ca^{2+} store, producing an initial Ca^{2+} signal that gradually rises with agonist concentration (red curve). As soon as this signal reaches the threshold level (dotted line), the process determining agonist-dependent delay of a cellular response, one stimulates IP_3 receptors of another type (IP_3R_{CICR}) in separated Ca^{2+} store and triggers CICR. This provides a significant amplification mechanism that finalizes transduction with a large and global Ca^{2+} signal (blue curve).

cut-off dose. Of course, the presented model is a simplification of the actual transduction process, and roles for other common contributors to intracellular Ca^{2+} signaling, including Ca^{2+} pumps, mitochondria, Ca^{2+} buffer as well as Ca^{2+}-dependent enzymes and ion channels, remain to be elucidated.

Acknowledgements

We thank Dr. V. Yu. Sysoeva for providing MSCs of the first passage. We are thankful to the Russian Science Foundation for support of studies of adrenergic and purinergic transduction (grant 18-14-0034) and P2Y receptors (grant 17-75-10127).

Author details

Polina D. Kotova, Olga A. Rogachevskaja, Marina F. Bystrova, Ekaterina N. Kochkina, Denis S. Ivashin and Stanislav S. Kolesnikov*

*Address all correspondence to: staskolesnikov@yahoo.com

Institute of Cell Biophysics of Russian Academy of Sciences, Pushchino, Moscow Region, Russia

References

[1] Kalinina NI, Sysoeva VY, Rubina KA, Parfenova YV, Tkachuk VA. Mesenchymal stem cells in tissue growth and repair. Acta Naturae. 2011;**3**:30-37

[2] Keating A. Mesenchymal stromal cells: New directions. Cell Stem Cell. 2012;**10**:709-716. DOI: 10.1016/j.stem.2012.05.015

[3] Baer PC. Adipose-derived mesenchymal stromal/stem cells: An update on their phenotype in vivo and in vitro. World journal of stem cells. 2014;**6**:256-265. DOI: 10.4252/wjsc.v6.i3.256

[4] Nordberg RC, Loboa EG. Our fat future: Translating adipose stem cell therapy. Stem Cells Translational Medicine. 2015;**4**:974-979. DOI: 10.5966/sctm.2015-0071

[5] Casiraghi F, Perico N, Cortinovis M, Remuzzi G. Mesenchymal stromal cells in renal transplantation: Opportunities and challenges. Nature Reviews. Nephrology. 2016;**12**:241-253. DOI: 10.1038/nrneph.2016.7

[6] Lou G, Chen Z, Zheng M, Liu Y. Mesenchymal stem cell-derived exosomes as a new therapeutic strategy for liver diseases. Experimental & Molecular Medicine. 2017;**49**:e346. DOI: 10.1038/emm.2017.63

[7] Scarfi S. Purinergic receptors and nucleotide processing ectoenzymes: Their roles in regulating mesenchymal stem cell functions. World Journal of Stem Cells. 2014;**6**:153-162. DOI: 10.4252/wjsc.v6.i2.153

[8] Forostyak O, Forostyak S, Kortus S, Sykova E, Verkhratsky A, Dayanithi G. Physiology of Ca^{2+} signalling in stem cells of different origins and differentiation stages. Cell Calcium. 2016;**59**:57-66. DOI: 10.1016/j.ceca.2016.02.001

[9] Penicaud L. Relationships between adipose tissues and brain: What do we learn from animal studies? Diabetes and Metabolism. 2010;**36**:S39-S44. DOI: 10.1016/S1262-3636 (10)70465-1

[10] Cavaliere F, Donno C, D'Ambrosi N. Purinergic signaling: A common pathway for neural and mesenchymal stem cell maintenance and differentiation. Frontiers in Cellular Neuroscience. 2015;**9**:211. DOI: 10.3389/fncel.2015.00211

[11] Glaser T, Cappellari AR, Pillat MM, Iser IC, Wink MR, Battastini AM, Ulrich H. Perspectives of purinergic signaling in stem cell differentiation and tissue regeneration. Purinergic Signal. 2012;**8**:523-537. DOI: 10.1007/s11302-011-9282-3

[12] Jiang LH, Hao Y, Mousawi F, Peng H, Yang X. Expression of P2 purinergic receptors in mesenchymal stem cells and their roles in extracellular nucleotide regulation of cell functions. Journal of Cellular Physiology. 2017;**232**:287-297. DOI: 10.1002/jcp.25484

[13] Ciciarello M, Zini R, Rossi L, Salvestrini V, Ferrari D, Manfredini R, Lemoli RM. Extracellular purines promote the differentiation of human bone marrow-derived mesenchymal stem cells to the osteogenic and adipogenic lineages. Stem Cells and Development. 2013;**22**:1097-1111. DOI: 10.1089/scd.2012.0432

[14] Gharibi B, Abraham AA, Ham J, Evans BA. Contrasting effects of A1 and A2b adenosine receptors on adipogenesis. International Journal of Obesity. 2012;**36**:397-406. DOI: 10.1038/ijo.2011.129

[15] Zimmermann H, Zebisch M, Strater N. Cellular function and molecular structure of ecto-nucleotidases. Purinergic Signal. 2012;**8**:437-502. DOI: 10.1007/s11302-012-9309-4

[16] Fredholm BB, IJzerman AP, Jacobson KA, Linden J, Muller CE. International Union of Basic and Clinical Pharmacology. LXXXI. Nomenclature and classification of adenosine receptors – An update. Pharmacological Reviews. 2011;**63**:1-34. DOI: 10.1124/pr.110.003285

[17] Fields RD, Burnstock G. Purinergic signalling in neuron-glia interactions. Nature Reviews Neuroscience. 2006;**7**:423-436. DOI: 10.1038/nrn1928

[18] Burnstock G. Purinergic signalling: From discovery to current developments. Experimental Physiology. 2014;**99**:16-34. DOI: 10.1113/expphysiol.2013.071951

[19] Saul A, Hausmann R, Kless A, Nicke A. Heteromeric assembly of P2X subunits. Frontiers in Cellular Neuroscience. 2013;**7**:250. DOI: 10.3389/fncel.2013.00250

[20] Samways DS, Li Z, Egan TM. Principles and properties of ion flow in P2X receptors. Frontiers in Cellular Neuroscience. 2014;**8**:6. DOI: 10.3389/fncel.2014.00006

[21] Cotecchia S. The α1-adrenergic receptors: Diversity of signaling networks and regulation. Journal of Receptor and Signal Transduction Research. 2010;**30**:410-419. DOI: 10.3109/10799893.2010.518152

[22] Cottingham C, Chen H, Chen Y, Peng Y, Wang Q. Genetic variations of a2-adrenergic receptors illuminate the diversity of receptor functions. Current Topics in Membranes. 2011;**67**:161-190. DOI: 10.1016/B978-0-12-384921-2.00008-2

[23] Lynch GS, Ryall JG. Role of beta-adrenoceptor signaling in skeletal muscle: Implications for muscle wasting and disease. Physiological Reviews. 2008;**88**:729-767. DOI: 10.1152/physrev.00028.2007

[24] Kotova PD, Sysoeva VY, Rogachevskaja OA, Bystrova MF, Kolesnikova AS, Tyurin-Kuzmin PA, Fadeeva JI, Tkachuk VA, Kolesnikov SS. Functional expression of adrenoreceptors in mesenchymal stromal cells derived from the human adipose tissue. Biochimica et Biophysica Acta. 2014;**1843**:1899-1908. DOI: 10.1016/j.bbamcr.2014.05.002

[25] Kalinina N, Kharlampieva D, Loguinova M, Butenko I, Pobeguts O, Efimenko A, Ageeva L, Sharonov G, Ischenko D, Alekseev D, Grigorieva O, Sysoeva V, Rubina K, Lazarev V, Govorun V. Characterization of secretomes provides evidence for adipose-derived mesenchymal stromal cells subtypes. Stem Cell Research & Therapy. 2015;**6**:221. DOI: 10.1186/s13287-015-0209-8

[26] Buvinic S, Briones R, Huidobro-Toro JP. P2Y1 and P2Y2 receptors are coupled to the NO/cGMP pathway to vasodilate the rat arterial mesenteric bed. British Journal of Pharmacology. 2002;**136**:847-856. DOI: 10.1038/sj.bjp.0704789

[27] Montiel M, de la Blanca EP, Jimenez E. P2Y receptors activate MAPK/ERK through a pathway involving PI3K/PDK1/PKC-zeta in human vein endothelial cells. Cellular Physiology and Biochemistry: International Journal of Experimental Cellular Physiology, Biochemistry and Pharmacology. 2006;**18**:123-134. DOI: 10.1159/000095180

[28] Luke TM, Hexum TD. UTP and ATP increase extracellular signal-regulated kinase 1/2 phosphorylation in bovine chromaffin cells through epidermal growth factor receptor transactivation. Purinergic Signal. 2008;**4**:323-330. DOI: 10.1007/s11302-008-9098-y

[29] Malaval C, Laffargue M, Barbaras R, Rolland C, Peres C, Champagne E, Perret B, Terce F, Collet X, Martinez LO. RhoA/ROCK I signalling downstream of the P2Y13 ADP-receptor controls HDL endocytosis in human hepatocytes. Cellular Signaling. 2009;**21**:120-127. DOI: 10.1016/j.cellsig.2008.09.016

[30] Berridge MJ. The inositol trisphosphate/calcium signaling pathway in health and disease. Physiological Reviews. 2016;**96**:1261-1296. DOI: 10.1152/physrev.00006.2016

[31] Xu SZ, Zeng F, Boulay G, Grimm C, Harteneck C, Beech DJ. Block of TRPC5 channels by 2-aminoethoxydiphenyl borate: A differential, extracellular and voltage-dependent effect. British Journal of Pharmacology. 2005;**145**:405-414. DOI: 10.1038/sj.bjp.0706197

[32] Mustafa T, Walsh J, Grimaldi M, Eiden LE. PAC1hop receptor activation facilitates catecholamine secretion selectively through 2-APB-sensitive Ca^{2+} channels in PC12 cells. Cellular Signaling. 2010;**22**:1420-1426. DOI: 10.1016/j.cellsig.2010.05.005

[33] Harteneck C, Gollasch M. Pharmacological modulation of diacylglycerol-sensitive TRPC3/6/7 channels. Current Pharmaceutical Biotechnology. 2011;**12**:35-41. DOI: 10.2174/138920111793937943

[34] Berg KA, Clarke WP, Sailstad C, Saltzman A, Maayani S. Signal transduction differences between 5-hydroxytryptamine type 2A and type 2C receptor systems. Molecular Pharmacology. 1994;**46**:477-484

[35] Baryshnikov SG, Rogachevskaja OA, Kolesnikov SS. Calcium signaling mediated by P2Y receptors in mouse taste cells. Journal of Neurophysiology. 2003;**90**:3283-3294. DOI: 10.1152/jn.00312.2003

[36] Petrel C, Kessler A, Dauban P, Dodd RH, Rognan D, Ruat M. Positive and negative allosteric modulators of the Ca^{2+}-sensing receptor interact within overlapping but not identical binding sites in the transmembrane domain. The Journal of Biological Chemistry. 2004;**279**:18990-18997. DOI: 10.1074/jbc.M400724200

[37] Berridge MJ, Bootman MD, Roderick HL. Calcium signaling: Dynamics, homeostasis and remodeling. Nature Reviews. Molecular Cell Biology. 2003;**4**:517-529. DOI: 10.1038/nrm1155

[38] Clapham DE. Calcium Signaling. Cell. 2007;**131**:1047-1058. DOI: 10.1016/j.cell.2007.11.028

[39] Iino M. Spatiotemporal dynamics of Ca^{2+} signaling and its physiological roles. Proceedings of the Japan Academy. Series B, Physical and Biological Sciences. 2010;**86**:244-256

[40] Thomas NL, Williams AJ. Pharmacology of ryanodine receptors and Ca^{2+}-induced Ca^{2+} release. Wiley Interdisciplinary Reviews: Membrane Transport and Signaling. 2012;**1**:383-397. DOI: 10.1002/wmts.34

[41] Ellis-Davies GC. Caged compounds: Photorelease technology for control of cellular chemistry and physiology. Nature Methods. 2007;**4**:619-628. DOI: 10.1038/nmeth1072

[42] Dupont G, Combettes L, Leybaert L. Calcium dynamics: Spatio-temporal organization from the subcellular to the organ level. International Review of Cytology. 2007;**261**:193-245. DOI: 10.1016/S0074-7696(07)61005-5

[43] Park JB, Lee CS, Jang JH, Ghim J, Kim YJ, You S, Hwang D, Suh P-G, Ryu SH. Phospholipase signalling networks in cancer. Nature Reviews. Cancer. 2012;**12**:782-792. DOI: 10.1038/nrc3379

[44] Kawamoto EM, Vivar C, Camandola S. Physiology and pathology of calcium signaling in the brain. Frontiers in Pharmacology. 2012;**3**:61. DOI: 10.3389/fphar.2012.00061

[45] Guimaraes S, Moura D. Vascular adrenoceptors: An update. Pharmacological Reviews. 2001;**2**:319-356

[46] Verkhratsky A, Burnstock G. Biology of purinergic signalling: Its ancient evolutionary roots, its omnipresence and its multiple functional significance. BioEssays: News and Reviews in Molecular, Cellular and Developmental Biology. 2014;**36**:697-705. DOI: 10.1002/bies.201400024

[47] Kotova PD, Bystrova MF, Rogachevskaja OA, Khokhlov AA, Sysoeva VY, Tkachuk VA, Kolesnikov SS. Coupling of P2Y receptors to Ca^{2+} mobilization in mesenchymal stromal cells from the human adipose tissue. Cell Calcium. 2018;**71**:1-14. DOI: 10.1016/j.ceca.2017.11.001

[48] Waldo GL, Harden TK. Agonist binding and Gq-stimulating activities of the purified human P2Y1 receptor. Molecular Pharmacology. 2004;**65**:426-436. DOI: 10.1124/mol.65.2.426

[49] von Kugelgen I, Hoffmann K. Pharmacology and structure of P2Y receptors. Neuropharmacology. 2016;**104**:50-61. DOI: 10.1016/j.neuropharm.2015.10.030

[50] Chhatriwala M, Ravi RG, Patel RI, Boyer JL, Jacobson KA, Harden TK. Induction of novel agonist selectivity for the ADP-activated P2Y1 receptor versus the ADP-activated P2Y12 and P2Y13 receptors by conformational constraint of an ADP analog. The Journal of Pharmacology and Experimental Therapeutics. 2004;**311**:1038-1043. DOI: 10.1124/jpet.104.068650

[51] Foskett JK, White C, Cheung KH, Mak DO. Inositol trisphosphate receptor Ca^{2+} release channels. Physiological Reviews. 2007;**87**:593-658. DOI: 10.1152/physrev.00035.2006

[52] Mikoshiba K. Role of IP_3 receptor signaling in cell functions and diseases. Advances in Biological Regulation. 2015;**57**:217-227. DOI: 10.1016/j.jbior.2014.10.001

[53] Taylor CW, da Fonseca PCA, Morris EP. IP_3 receptors: The search for structure. Trends in Biochemical Science. 2004;**29**:210-219. DOI: 10.1016/j.tibs.2004.02.010

[54] Mak DO, Foskett JK. Inositol 1,4,5-trisphosphate receptors in the endoplasmic reticulum: A single-channel point of view. Cell Calcium. 2015;**58**:67-78. DOI: 10.1016/j.ceca.2014.12.008

[55] Alzayady KJ, Wang L, Chandrasekhar R, Wagner LE 2nd, Van Petegem F, Yule DI. Defining the stoichiometry of inositol 1,4,5-trisphosphate binding required to initiate Ca^{2+} release. Science Signaling. 2016;**9**:ra35. DOI: 10.1126/scisignal.aad6281

[56] Phinney DG. Functional heterogeneity of mesenchymal stem cells: Implications for cell therapy. Journal of Cellular Biochemistry. 2012;**113**:2806-2812. DOI: 10.1002/jcb.24166

[57] Galle J, Hoffmann M, Krinner A. Mesenchymal stem cell heterogeneity and ageing in vitro: A model approach. In: Geris L, editor. Computational Modeling in Tissue Engineering. Berlin, Heidelberg: Springer Berlin Heidelberg; 2013. pp. 183-205. DOI: 10.1007/8415_2012_116

[58] Prakriya M, Solaro CR, Lingl CJ. $[Ca^{2+}]_i$ elevations detected by BK channels during Ca^{2+} influx and muscarine-mediated release of Ca^{2+} from intracellular stores in rat chromaffin cells. Journal of Neuroscience. 1996;**16**:4344-4359. DOI: 10.1523/JNEUROSCI.16-14-04344.1996

[59] Faas GC, Karacs K, Vergara JL, Mody I. Kinetic properties of DM-Nitrophen binding to calcium and magnesium. Biophysical Journal. 2005;**88**:4421-4433. DOI: 10.1529/biophysj.104.057745

IntechOpen